

## Electronic Supplementary Information

### Dual Emitting Ag<sub>35</sub> Nanocluster Protected by 2-Pyrene Imine Thiol

Arijit Jana<sup>a,b</sup>, Papri Chakraborty<sup>a</sup>, Wakeel Ahmed Dar<sup>a</sup>, Sourov Chandra<sup>b</sup>, Esmā Khatun<sup>a</sup>, M. P. Kannan<sup>a</sup>, Robin H. A. Ras<sup>b,c</sup>, Thalappil Pradeep<sup>a,\*</sup>.

<sup>a</sup>DST Unit of Nanoscience (DST UNS) and Thematic Unit of Excellence (TUE), Department of Chemistry, Indian Institute of Technology, Madras, Chennai – 600036, India.

<sup>b</sup>Department of Applied Physics, Aalto University School of Science, Puumiehenkuja 2, 02150 Espoo, Finland.

<sup>c</sup>Department of Bioproducts and Biosystems, Aalto University School of Chemical Engineering, 02150, Espoo, Finland.

\*Email: [pradeep@iitm.ac.in](mailto:pradeep@iitm.ac.in)

Items	Descriptions	Page No.
1)	Experimental section	2
2)	Instrumentation	3-6
Fig. S1	<sup>1</sup> H NMR spectrum of the 2-PIT ligand in CDCl <sub>3</sub> solvent	7
Fig. S2	<sup>13</sup> C { <sup>1</sup> H} NMR spectrum of 2-PIT ligand	8
Fig. S3	Unit cell packing of 2-PIT ligand showing different intermolecular interactions	9
Fig. S4	UV-Visible absorption spectrum and ESI-MS spectrum of Ag <sub>18</sub> NCs	10
Fig. S5	Optical images of the vial during the reaction including UV-Visible spectra of the different intermediates	11
Fig. S6	<sup>31</sup> P { <sup>1</sup> H} NMR spectrum of Ag <sub>35</sub> NC	12
Fig. S7	XPS spectra of the 2-PIT ligand having each component peak fitting	13
Fig. S8	XPS spectra of Ag <sub>35</sub> NCs having each component peak fitting	14
Fig. S9	Optical microscopic images of the NC crystals and its weak diffraction spots	15
Fig S10	IR spectra of 2-PIT ligand and Ag <sub>35</sub> nanocluster	16

## **Experimental Section:**

### **1) Chemicals used:**

Pyrenecarboxaldehyde and 2-aminothiophenol were purchased from Sigma-Aldrich and Avra, India chemicals, respectively. Silver nitrate ( $\text{AgNO}_3$ ) was purchased from Rankem chemicals. Sodium borohydride ( $\text{NaBH}_4$ , 98%) and triphenylphosphine (TPP) were purchased from Aldrich chemicals. All the chemicals were commercially available and used as such without any further purification. Solvent grade dichloromethane (DCM), chloroform ( $\text{CHCl}_3$ ), n-hexane, and methanol (99.5%) were purchased from Rankem chemicals and Finar, India respectively. Milli-Q water was used as the source of water for  $\text{Ag}_{18}$  nanocluster synthesis. Deuterated solvent ( $\text{CDCl}_3$ ) was purchased from Aldrich chemical.

### **2) Synthesis of $[\text{Ag}_{18}(\text{PPh}_3)_{10}\text{H}_{16}]^{+2}\text{NCs}$ :**

$\text{Ag}_{18}$  NCs were synthesized by following the previous literature.<sup>[S1]</sup> In Brief, at room temperature, 20 mg silver nitrate ( $\text{AgNO}_3$ ) was dissolved in 5 mL methanol and 8 mL  $\text{CHCl}_3$  under ultrasonic condition. After that, 70 mg triphenylphosphene (TPP) was dissolved in 2 ml methanol and added to it under stirring condition. After 20 min of reaction, 6.5 mg  $\text{NaBH}_4$ , dissolved in 0.75 mL milli-Q water, was added to it quickly. After addition of  $\text{NaBH}_4$ , reaction mixture became clean yellow solution which gradually converted to dark brownish solution and finally became dark green solution which indicated the formation of  $\text{Ag}_{18}$  NC. After 3.5 hour reaction, mixed solvent were removed at reduced pressure. Dark greenish nanocluster was dissolved in cold water to remove excess  $\text{NaBH}_4$  and  $\text{AgNO}_3$ . Finally, dark greenish  $\text{Ag}_{18}$  nanocluster was extracted using methanol. Formation of the NC was confirmed using UV-Vis spectroscopy and mass spectrometry, as shown in Fig. S4. The yield of the reaction was 25 % in terms of silver.

### **3) Synthesis of 2 pyrene imine thiol ligand:**

1000 mg (4.35 mM) of pyrene aldehyde was mixed with 762 mg (6.09 mM, 1.4 eq) of 2 amino thiophenol in an argon atmosphere. After 20 min of solid state mixing, 20 ml methanol and 10 ml ethanol was mixed with them and put for 4 hour refluxion at 60 °C. After the reaction, yellow color ligand was filtered using Whatman 42 filter paper and washed several times with excess ethanol and methanol to remove the excess starting materials. (Yield of the product: 1.58 gm, 90 %, yellow color). 2-PIT ligands were non emissive in both solid state as well as in solution.

**$^1\text{H NMR}$  ( $\text{CDCl}_3$ , 500 MHz)  $\delta$  = 3.45 (s, 1H, S-H); 6.62 (m, 2H, Ar-H); 7.15 (m, 2H, Ar-H); 7.54 (dt, 1H, Pyr-H); 8.1 (m, 4H, Pyr-H); 8.27 (m, 4H, Pyr-H); 8.47 (t, 1H NC-H).**

**$^{13}\text{C}$   $\{^1\text{H}\}$  NMR ( $\text{CDCl}_3$ , 125 MHz)  $\delta$  = 168.16, 136.62, 132.99, 131.29, 130.65, 129.17, 128.97, 128.55, 127.19, 127.05, 126.79, 126.59, 126.42, 126.33, 126.03, 125.74, 125.28, 124.70, 123.47, 122.95, 121.43, 118.14, 115.21 ppm.**

#### **4) Synthesis of Ag<sub>35</sub> nanocluster:**

Ag<sub>35</sub> nanocluster was prepared using modified ligand exchange reaction. About 15 mg purified Ag<sub>18</sub> nanocluster in 20 ml methanol was mixed with 4.5-5 mg 2-PIT ligand dissolved in 2-3 ml DCM solvent in dark condition. After 1 hour reaction at room temperature, greenish color Ag<sub>18</sub> nanocluster converted to a dark reddish color solution. After 24 hour reaction solution became wine red. Based on the UV-Vis absorption spectrum of these intermediates shown in Fig.S5b, which infers that these are mixed Ag-thiolate and Ag-phosphine complexes. The reaction was continued upto 48 hour which lead to the formation of dark violet colored Ag<sub>35</sub> nanocluster. After that, the solvents were evaporated in rotary evaporator and the cluster was washed several times with ethanol and water to remove excess ligands and silver precursors. Purified Ag<sub>35</sub> nanocluster, soluble in dichloromethane and chloroform, was used for further studies.

#### **5) Crystallization of Ag<sub>35</sub> nanocluster:**

30 mg purified Ag<sub>35</sub> nanocluster in 2.5 ml DCM solvent, layered with 0.75-1 ml hexane, led to the formation of cubical nanocluster crystals.

### **Instrumentation:**

#### **1) UV Visible spectroscopic measurements:**

Perkin Elmer Lambda 365 UV Visible spectrophotometer was used to study the optical absorption spectra for the clusters in the wavelength region of 200 to 1100 nm.

#### **2) ESI MS spectra:**

Mass spectrum of 2-pyrene imine thiol (2-PIT) was recorded using an ion trap Thermo Scientific LTQ XL mass spectrometer. Mass spectrum of Ag<sub>18</sub> and Ag<sub>35</sub> NCs were collected using Waters Synapt G2Si HDMS instrument. Both Ag<sub>18</sub> and Ag<sub>35</sub> NCs were measured in the positive ion mode. All the fragmentation experiments were recorded by varying the collision energy in the trap and transfer chambers of the same instrument. An optimized condition of capillary voltage 3 kV, spray current 100 nA, cone voltage 1 kV were used to record the mass spectrum of the cluster.

#### **3) Microscopic characterizations:**

##### **a) Optical imaging:**

All the optical microscopic images of the crystal were collected in 10X magnification using LEICA optical microscope equipped with LAS V4.8 software.

##### **b) TEM imaging:**

Size distribution of the NCs were recorded using Transmission electron microscopy, which was recorded at -40°C by using a JEOL 3010 high resolution transmission electron microscope operated at 200 kV. A Gatan multistage CCD camera was used to record the image.

**c) SEM EDS study:**

SEM EDS measurements were performed using Verios G4 UC, Thermo Scientific HRSEM instrument.

**4) Photoluminescence spectra:**

Photoluminescence spectra were measured using Jobin Yvon Nanolog spectrofluorometer equipped with Fluorescence V3 software.

**5) XPS study:**

X ray photoelectron spectroscopy were recorded using ESCA probe TPD equipped with polychromatic Mg K $\alpha$  X ray source ( $h\nu = 1253.6$  eV). DCM soluble cluster solution were spotted onto the XPS grid for the measurements.

**6) FTIR spectroscopic measurements:**

IR spectra of the 2-PIT ligand and Ag<sub>35</sub> NCs were recorded using Perkin Elmer FT-IR spectrometer.

**7) Single crystal XRD measurements:**

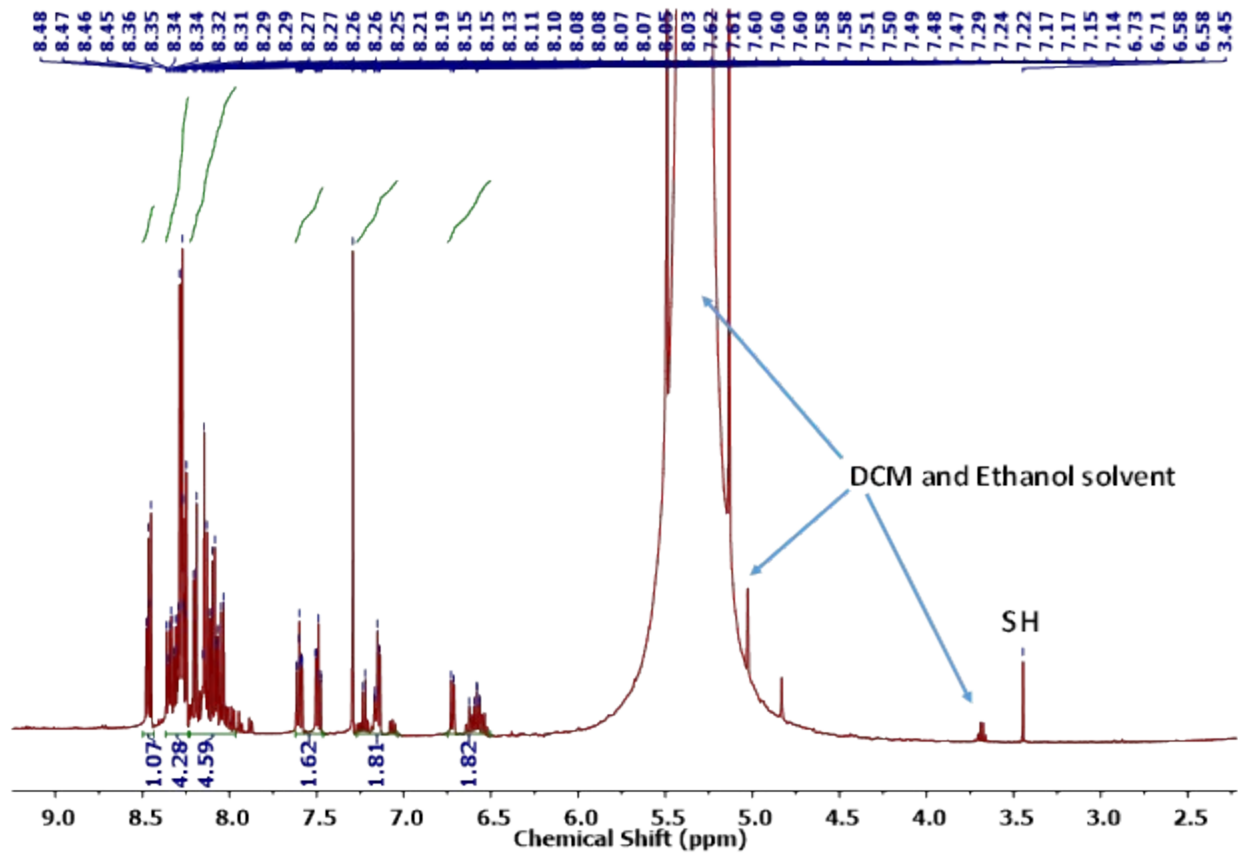
Single crystal X-ray diffraction data was collected using Bruker D8 VENTURE SC-XRD diffractometer, equipped with monochromatic Mo(K $\alpha$ ) ( $\lambda = 0.71073$ ) radiation at 296K. The structure was solved using SHELXL-2018 (Sheldrick, 2018) and refined using full matrix least squares techniques. The program APEX3-S SAINT V8.37A (Bruker-2016) was used for integrating the frames. Hydrogen, carbon atoms were fixed at calculated positions and refined model. All the molecular structures, interaction and molecular packing were obtained using the Mercury software (Version 3.9).

Table S1. Crystal data and structure refinement for 2-pyrene imine thiol.

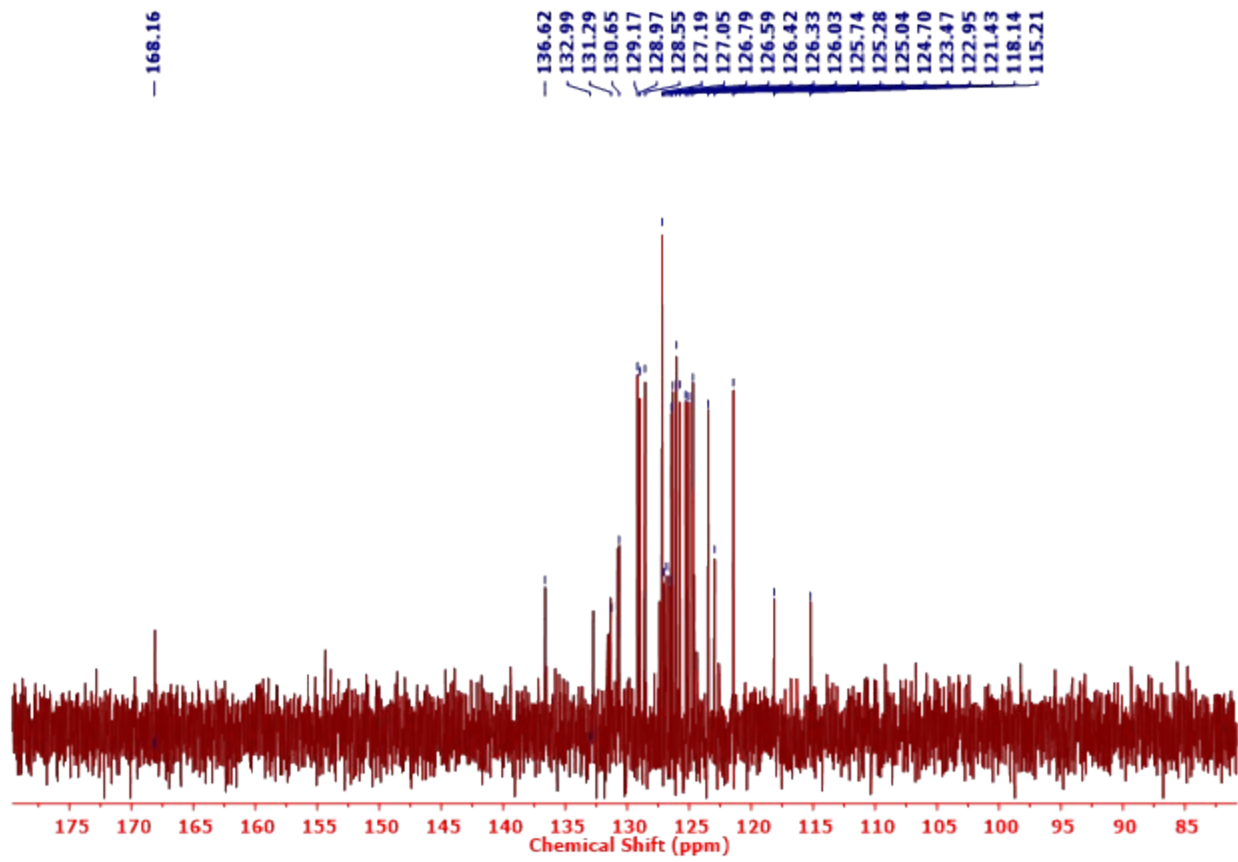
Identification code	AJ/2-PIT	
Empirical formula	C <sub>23</sub> H <sub>13</sub> N S	
Formula weight	335.40	
Temperature	296(2) K	
Wavelength	0.71073 Å	
Crystal system	Monoclinic	
Space group	P2 <sub>1</sub> /c	
Unit cell dimensions	a = 21.4278(11) Å	α = 90°.
	b = 4.9469(2) Å	β = 107.158(2)°.
	c = 15.5164(8) Å	γ = 90°.
Volume	1571.56(13) Å <sup>3</sup>	
Z	4	
Density (calculated)	1.418 Mg/m <sup>3</sup>	
Absorption coefficient	0.210 mm <sup>-1</sup>	
F(000)	696	
Crystal size	0.150 x 0.150 x 0.100 mm <sup>3</sup>	
Theta range for data collection	3.409 to 24.993°.	
Index ranges	-25 ≤ h ≤ 25, -5 ≤ k ≤ 5, -18 ≤ l ≤ 18	
Reflections collected	31947	
Independent reflections	2751 [R(int) = 0.0901]	
Completeness to theta = 24.993°	99.7 %	
Absorption correction	Semi-empirical from equivalents	
Max. and min. transmission	0.7445 and 0.6331	
Refinement method	Full-matrix least-squares on F <sup>2</sup>	
Data / restraints / parameters	2751 / 0 / 226	
Goodness-of-fit on F <sup>2</sup>	1.150	
Final R indices [I > 2σ(I)]	R1 = 0.0679, wR2 = 0.1488	
R indices (all data)	R1 = 0.0888, wR2 = 0.1600	
Extinction coefficient	n/a	
Largest diff. peak and hole	0.407 and -0.319 e.Å <sup>-3</sup>	

Table S2. Atomic coordinates ( $\times 10^4$ ) and equivalent isotropic displacement parameters ( $\text{\AA}^2 \times 10^3$ ) for 1.  $U(\text{eq})$  is defined as one third of the trace of the orthogonalized  $U^{ij}$  tensor.

	x	y	z	$U(\text{eq})$
C(1)	5785(2)	8045(7)	4465(2)	39(1)
C(2)	5228(2)	9511(7)	4019(2)	44(1)
C(3)	5266(2)	11345(7)	3382(2)	46(1)
C(4)	5852(2)	11734(7)	3165(2)	49(1)
C(5)	6398(2)	10249(7)	3592(2)	48(1)
C(6)	6370(2)	8388(6)	4239(2)	38(1)
C(7)	6721(2)	5275(6)	5304(2)	37(1)
C(8)	7134(2)	3299(7)	5916(2)	37(1)
C(9)	6941(2)	2449(7)	6661(2)	46(1)
C(10)	7285(2)	572(8)	7258(2)	49(1)
C(11)	7844(2)	-614(7)	7152(2)	42(1)
C(12)	8210(2)	-2596(8)	7763(2)	54(1)
C(13)	8734(2)	-3793(8)	7625(2)	55(1)
C(14)	8952(2)	-3137(7)	6867(2)	47(1)
C(15)	9491(2)	-4386(8)	6709(3)	56(1)
C(16)	9691(2)	-3689(8)	5976(3)	60(1)
C(17)	9361(2)	-1767(8)	5376(3)	53(1)
C(18)	8819(2)	-433(7)	5502(2)	41(1)
C(19)	8610(2)	-1135(6)	6258(2)	38(1)
C(20)	8050(2)	154(6)	6395(2)	36(1)
C(21)	7702(2)	2142(6)	5779(2)	34(1)
C(22)	7941(2)	2818(7)	5032(2)	40(1)
C(23)	8469(2)	1587(7)	4909(2)	44(1)
N(1)	6883(1)	6787(6)	4721(2)	42(1)
S(1)	5902(1)	5684(2)	5314(1)	46(1)



**Fig. S1:**  $^1\text{H}$  NMR spectrum of 2-pyrene imine thiol ligand in  $\text{CDCl}_3$  solvent. (DCM, ethanol peaks are due to impurity).



**Fig. S2:**  $^{13}\text{C}$   $\{^1\text{H}\}$  NMR spectrum of 2-pyrene imine thiol ligand in  $\text{CDCl}_3$  solvent.

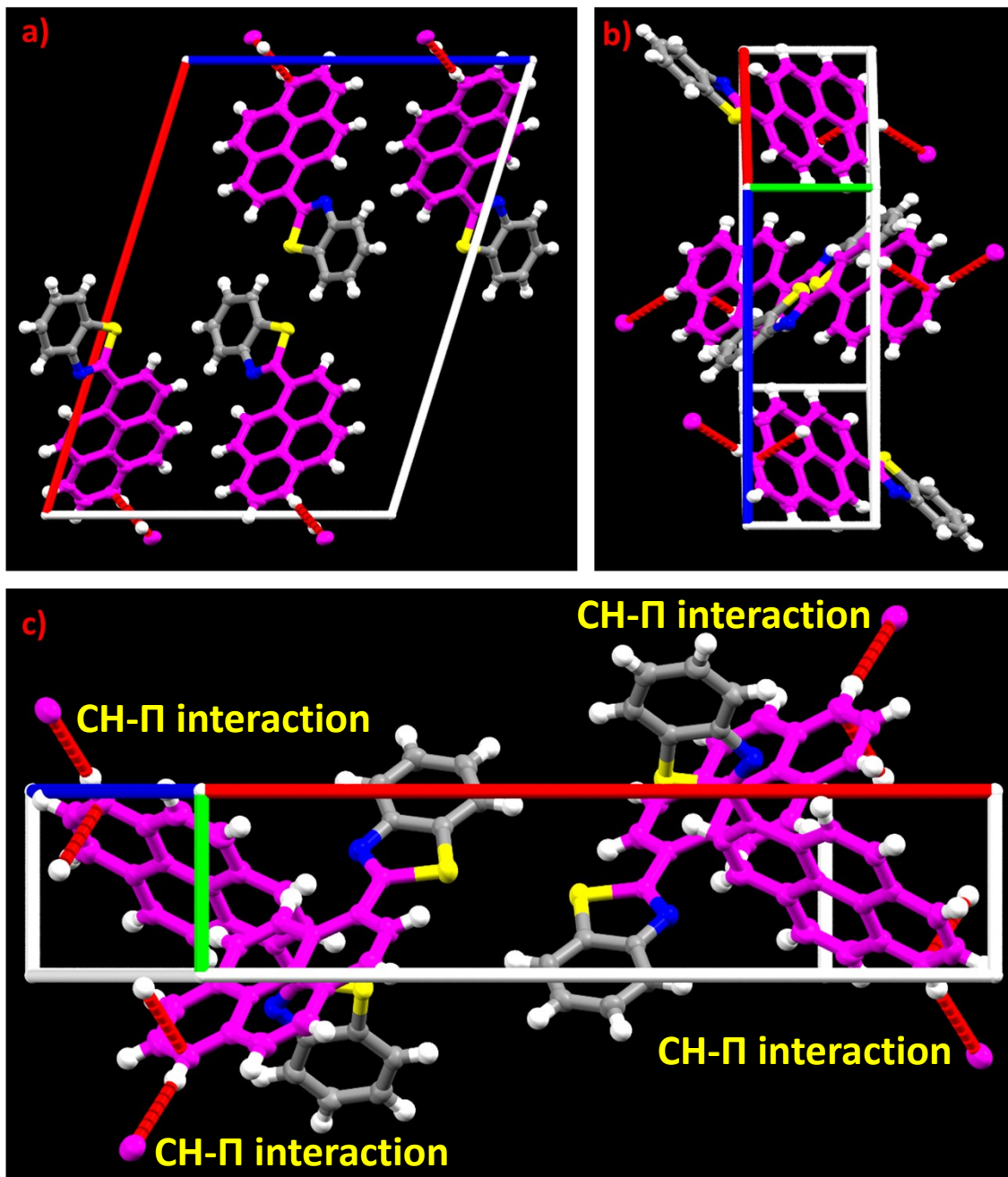


**Fig. S3:** a, b, c) Single crystal unit cell packing of 2-PIT molecule in three different orientations. Several C-H - $\pi$  intermolecular interactions leading to the crystallization are shown here.

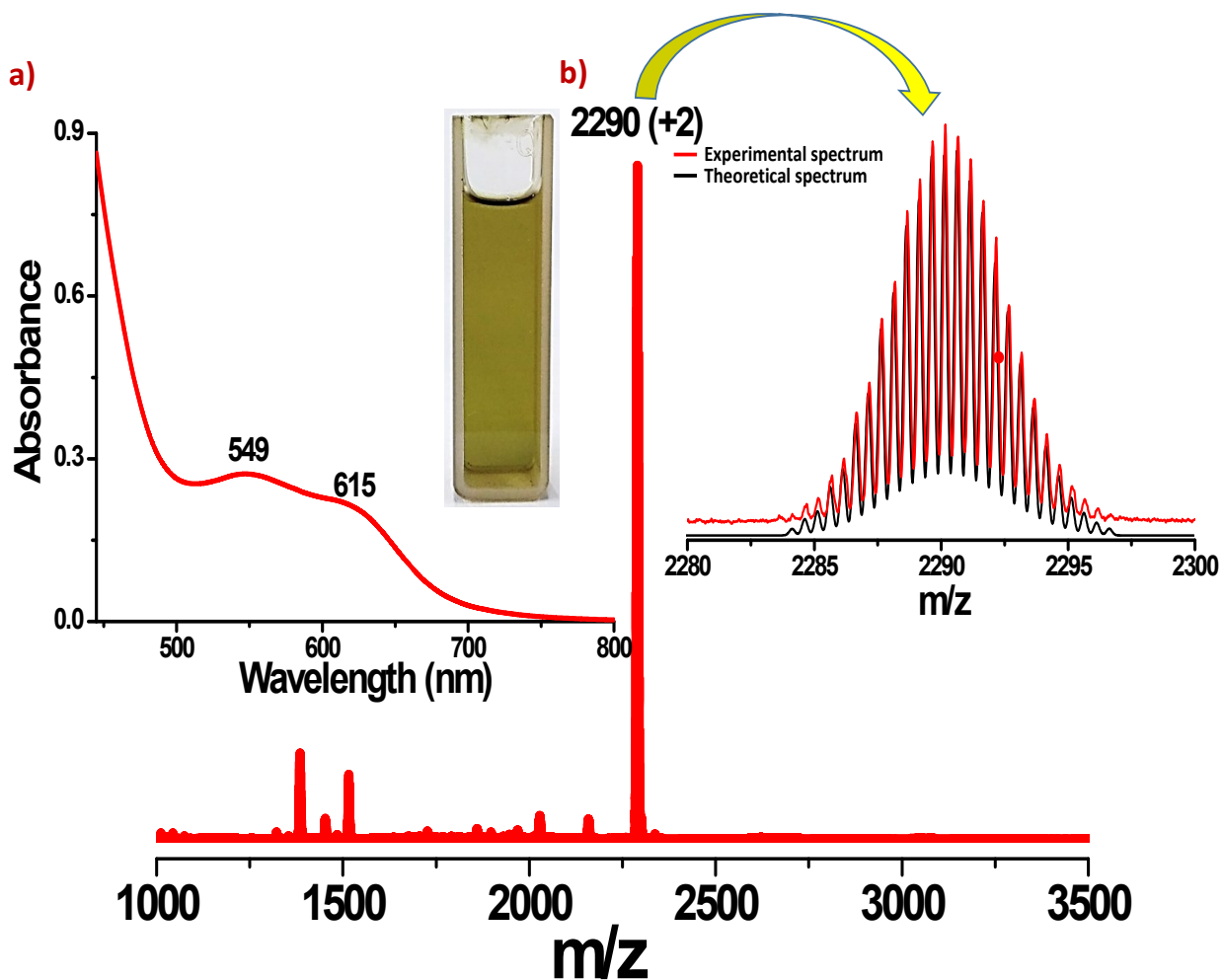


**Fig. S4:** a) UV-Visible absorption spectrum of  $\text{Ag}_{18}$  NC in methanol (inset digital image of the nanocluster); b) positive mode ESI-MS spectrum of the NC (inset shows experimental and theoretical spectrum).

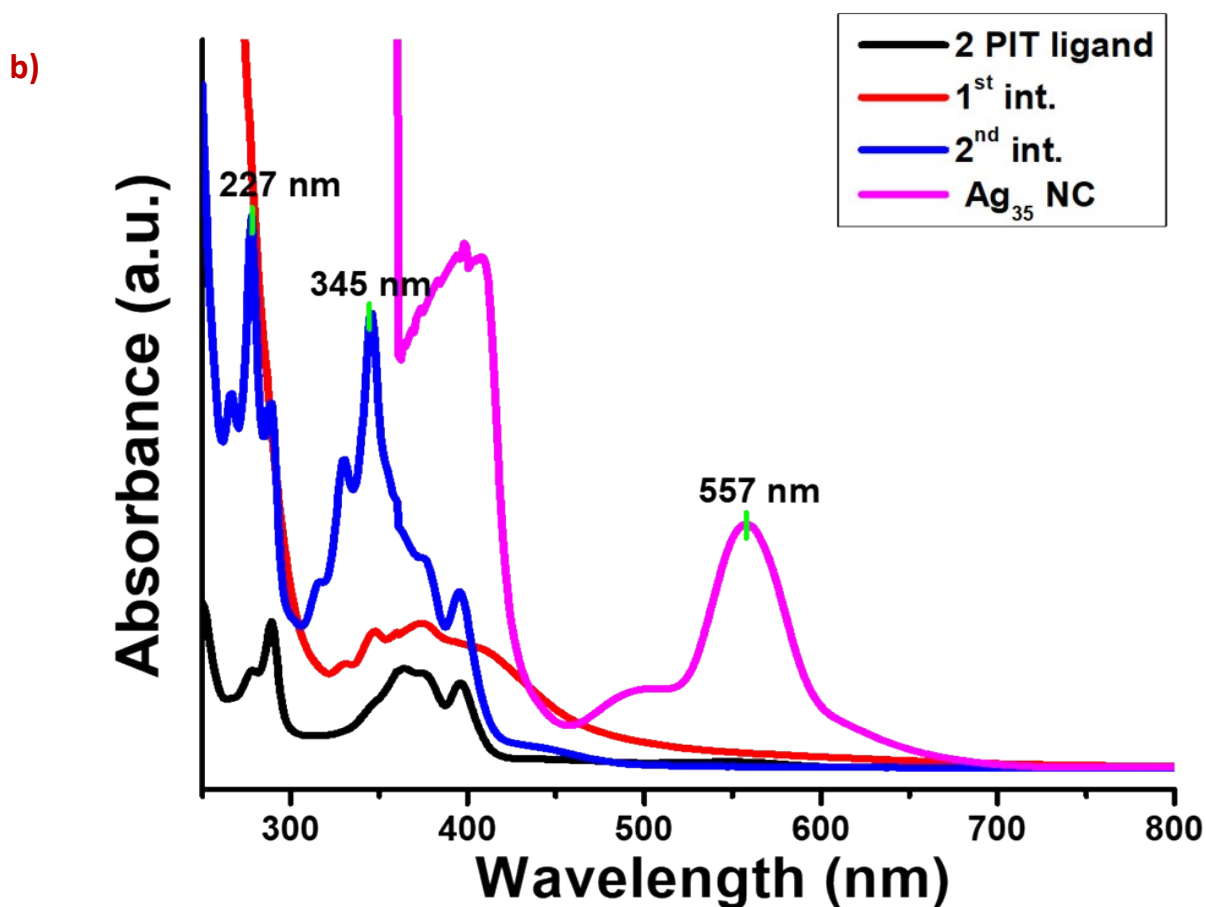
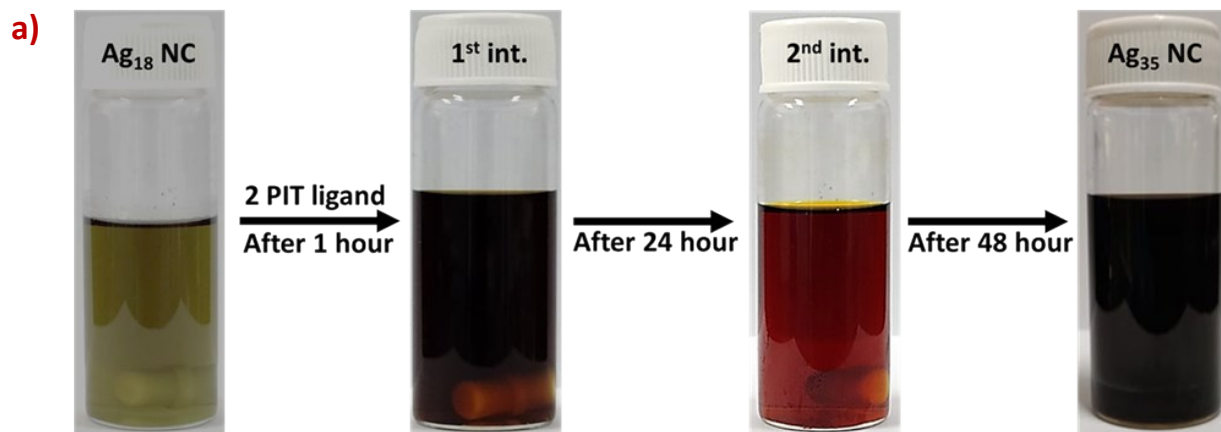


**Fig. S5:** a) Photographs of the reaction mixtures during the course of the reaction; b) UV-Vis absorption spectrum of the ligand, intermediates and Ag<sub>35</sub> NC. (emergence of the characteristic peak at 557 nm indicated the formation of Ag<sub>35</sub> NC).

Ag<sub>35</sub> NC

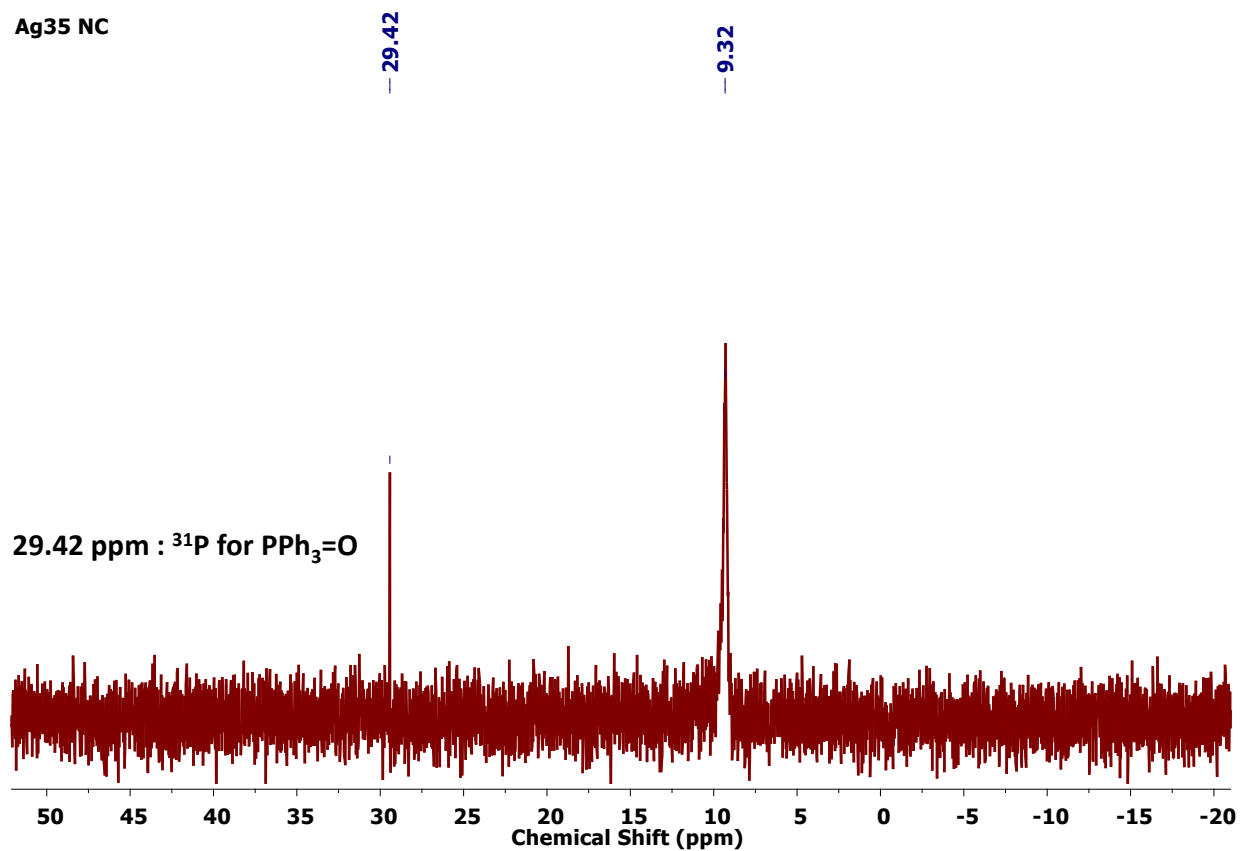


**Fig. S6:** <sup>31</sup>P {<sup>1</sup>H} NMR spectrum of Ag<sub>35</sub> nanocluster in CDCl<sub>3</sub> solvent (broad NMR peak at 9.32 ppm indicating phosphorous of PPh<sub>3</sub> binding with cluster).

### XPS analysis:

The XPS spectra are shown in Fig. S7 and S8 (Table S3) of the ligand and Ag<sub>35</sub> NC, respectively. Among the four peaks of Ag<sub>35</sub> NC, two peaks at 284.8 and 286.6 eV are comparable with the two peaks at 284.8 and 286.3 eV of the C 1s region of the 2-PIT ligand, which suggests the binding of the 2-PIT ligand. The two other peaks of the C 1s region at 288.2 and 289.4 eV are due to the two types of TPP ligands. The decrease in the binding energy of the N 1s and S 2p regions in the Ag<sub>35</sub> NC, compared to the 2-PIT ligand, is probably due to the electron back donation from the metal core to the N and S end of the ligand. The higher electronegativity of N and S compared to Ag is also the reason behind it. The binding energy of 368.4 and 374.5 eV for the Ag 3d region suggests the metallic state of silver.

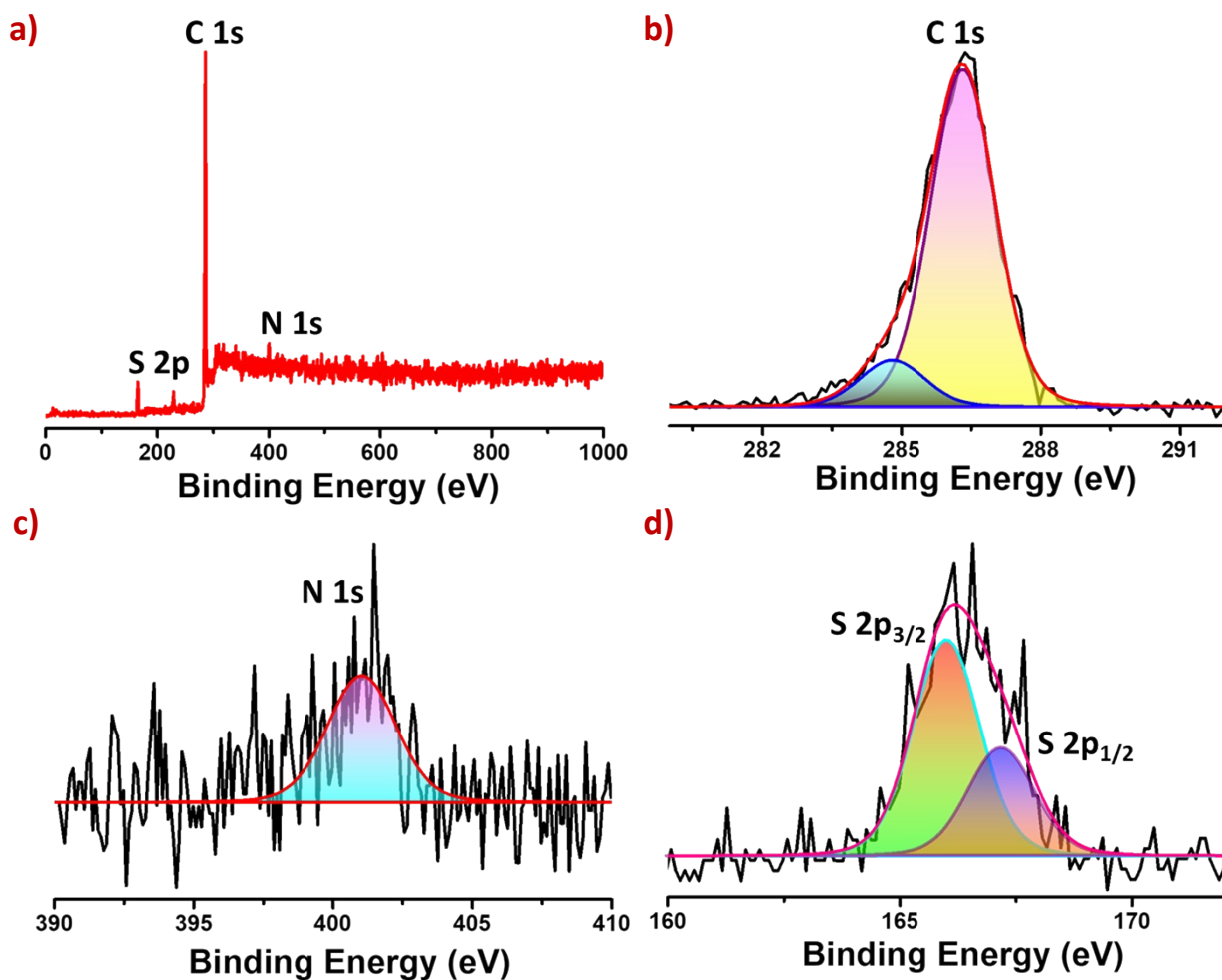


**Fig. S7:** XPS spectra of 2-PIT ligand a) survey spectrum indicating C, N and S characteristic peak; peak fitting of b) C 1s showing two fitted peaks; c) N 1s and, d) S 2p regions.

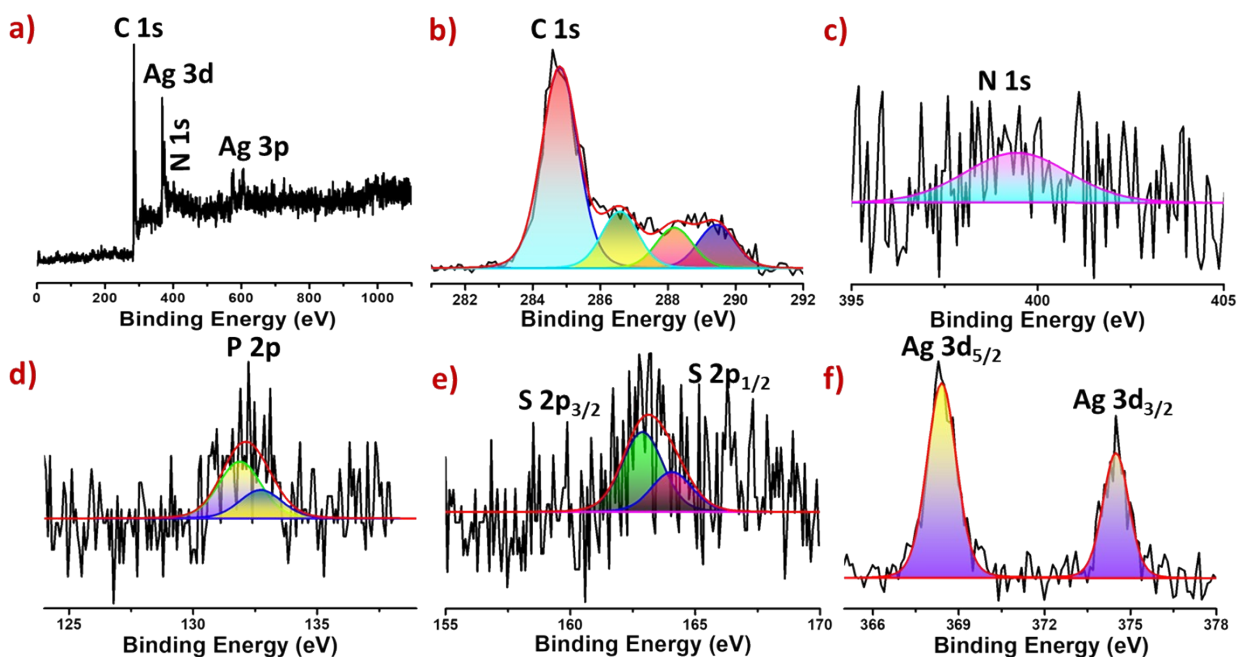


**Fig. S8:** XPS spectra of the Ag<sub>35</sub> NCs; a) survey spectrum of the NCs indicating different regions; peak fitting of the b) C 1s indicating four fitted peaks; c) N 1s; d) P 2p; e) S 2p; f) Ag 3d regions.

**Table S3:** Comparative binding energy of Ag<sub>35</sub> NC and 2-PIT ligand in different spectral region.

Spectral regions	Binding energy (Ag <sub>35</sub> NC)	Binding energy (2-PIT ligand)
C 1s	284.8 eV	284.8 eV
	286.6 eV	286.3 eV
	288.2 eV	
	289.4 eV	
N 1s	399.4 eV	401 eV
S 2p	162.8 eV (S 2p <sub>3/2</sub> )	166 eV (S 2p <sub>3/2</sub> )
	164 eV (S 2p <sub>1/2</sub> )	167.1 eV (S 2p <sub>1/2</sub> )
P 2p	131.8 eV	
	132.7 eV	
Ag 3d	368.4 eV (Ag 3d <sub>5/2</sub> )	
	374.5 eV (Ag 3d <sub>3/2</sub> )	

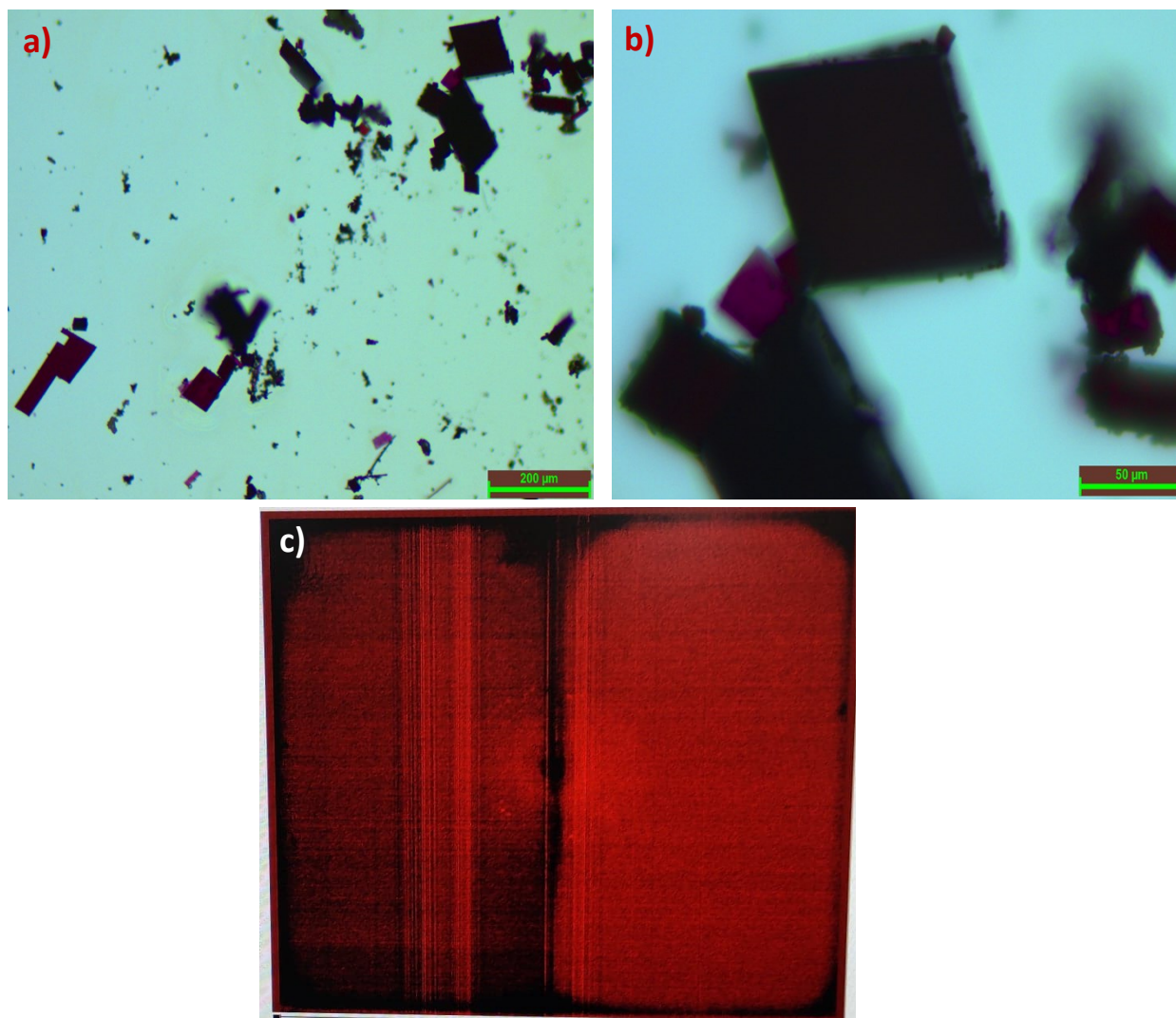


**Fig. S9:** a) Large area optical microscopic images of the nanocluster crystals; b) magnified image under bright field; c) photographs of weak single-crystal X-ray diffraction spots.

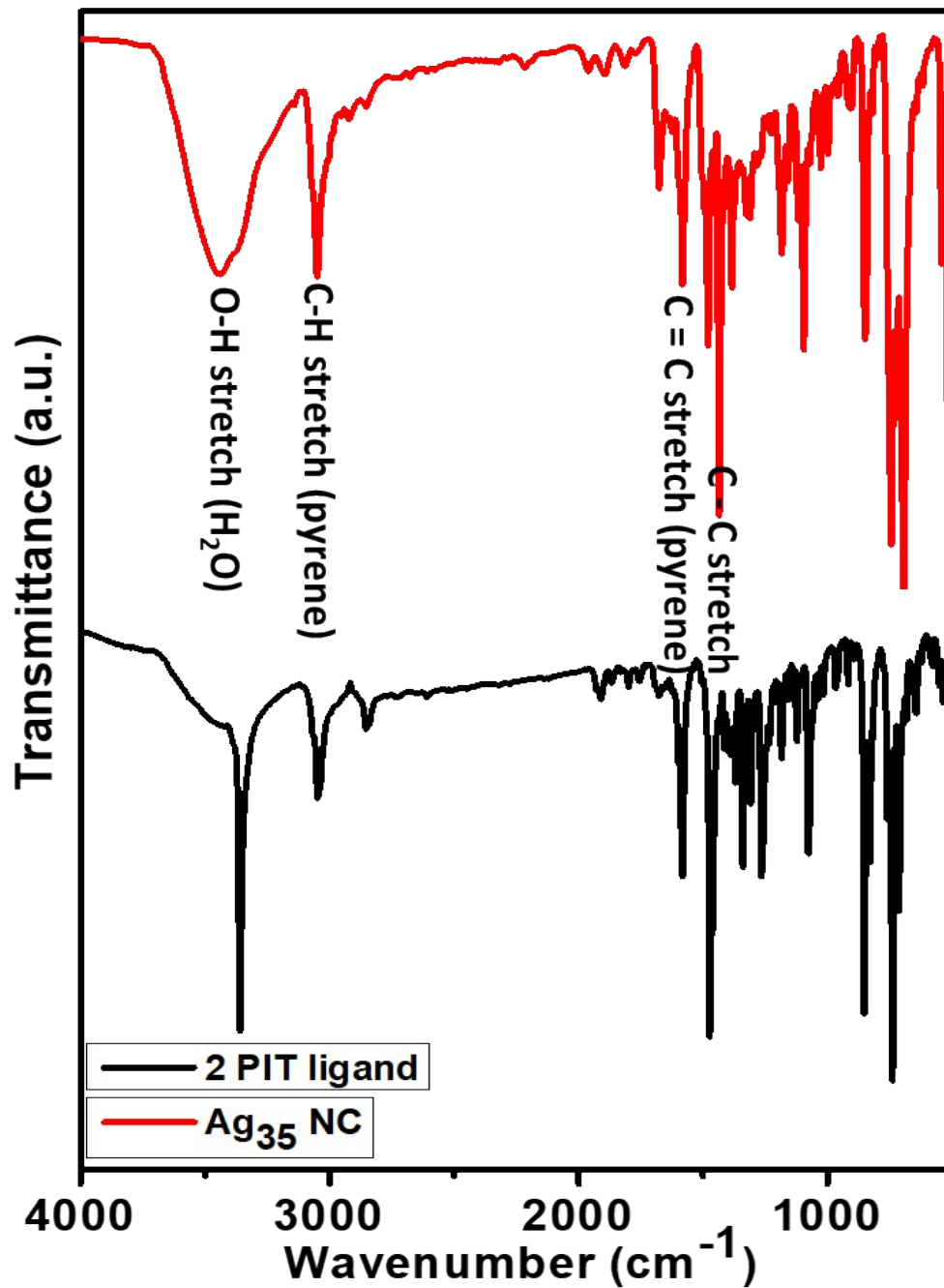


**Fig. S10:** The IR spectra of 2-PIT ligand and  $\text{Ag}_{35}\text{ NC}$  (pyrene C-H, C=C and  $\text{H}_2\text{O}$  stretching peaks are marked here).

**References:**

- S1 O. M. Bakr, Megalamane S. Bootharaju, Raju Dey, Lieven E. Gevers, Mohamed N. Hedhili, Jean-Marie Basset, *J. Am. Chem. Soc.*, 2016, **138**, 13770–13773.